

Taylor & Francis
Taylor & Francis Group

Inhalation Toxicology

International Forum for Respiratory Research

ISSN: 0895-8378 (Print) 1091-7691 (Online) Journal homepage: http://www.tandfonline.com/loi/iiht20

Effects of cigarette smoke, cessation and switching to a candidate modified risk tobacco product on the liver in Apoe$^{-/-}$ mice – a systems toxicology analysis

Giuseppe Lo Sasso, Bjoern Titz, Catherine Nury, Stéphanie Boué, Blaine Phillips, Vincenzo Belcastro, Thomas Schneider, Sophie Dijon, Karine Baumer, Daruisz Peric, Remi Dulize, Ashraf Elamin, Emmanuel Guedj, Ansgar Buettner, Patrice Leroy, Samuel Kleinhans, Gregory Vuillaume, Emilija Veljkovic, Nikolai V. Ivanov, Florian Martin, Patrick Vanscheeuwijck, Manuel C. Peitsch & Julia Hoeng

To cite this article: Giuseppe Lo Sasso, Bjoern Titz, Catherine Nury, Stéphanie Boué, Blaine Phillips, Vincenzo Belcastro, Thomas Schneider, Sophie Dijon, Karine Baumer, Daruisz Peric, Remi Dulize, Ashraf Elamin, Emmanuel Guedj, Ansgar Buettner, Patrice Leroy, Samuel Kleinhans, Gregory Vuillaume, Emilija Veljkovic, Nikolai V. Ivanov, Florian Martin, Patrick Vanscheeuwijck, Manuel C. Peitsch & Julia Hoeng (2016) Effects of cigarette smoke, cessation and switching to a candidate modified risk tobacco product on the liver in Apoe$^{-/-}$ mice – a systems toxicology analysis, Inhalation Toxicology, 28:5, 226-240, DOI: 10.3109/08958378.2016.1150368

To link to this article: http://dx.doi.org/10.3109/08958378.2016.1150368

View supplementary material

Published online: 30 Mar 2016.

Submit your article to this journal

Article views: 97

View related articles

View Crossmark data

Full Terms & Conditions of access and use can be found at
http://www.tandfonline.com/action/journalInformation?journalCode=iiht20

Download by: [PMP S A], [Bjoern Titz] **Date:** 28 April 2016, At: 08:38

Inhalation Toxicology

http://tandfonline.com/iiht
ISSN: 0895-8378 (print), 1091-7691 (electronic)

Inhal Toxicol, 2016; 28(5): 226–240
© 2016 Informa UK Limited, trading as Taylor & Francis Group. DOI: 10.3109/08958378.2016.1150368

Taylor & Francis
Taylor & Francis Group

RESEARCH ARTICLE

Effects of cigarette smoke, cessation and switching to a candidate modified risk tobacco product on the liver in *Apoe*$^{-/-}$ mice – a systems toxicology analysis

Giuseppe Lo Sasso[1]*, Bjoern Titz[1]*, Catherine Nury[1]*, Stéphanie Boué[1]*, Blaine Phillips[2]*, Vincenzo Belcastro[1], Thomas Schneider[1], Sophie Dijon[1], Karine Baumer[1], Daruisz Peric[1], Remi Dulize[1], Ashraf Elamin[1], Emmanuel Guedj[1], Ansgar Buettner[3], Patrice Leroy[1], Samuel Kleinhans[1], Gregory Vuillaume[1], Emilija Veljkovic[1], Nikolai V. Ivanov[1], Florian Martin[1], Patrick Vanscheeuwijck[1], Manuel C. Peitsch[1], and Julia Hoeng[1]

[1]*Philip Morris International Research and Development, Neuchatel, Switzerland,* [2]*Philip Morris International Research Laboratories, Singapore, Singapore, and* [3]*Histovia GmbH, Overath, Germany*

Abstract

The liver is one of the most important organs involved in elimination of xenobiotic and potentially toxic substances. Cigarette smoke (CS) contains more than 7000 chemicals, including those that exert biological effects and cause smoking-related diseases. Though CS is not directly hepatotoxic, a growing body of evidence suggests that it may exacerbate pre-existing chronic liver disease. In this study, we integrated toxicological endpoints with molecular measurements and computational analyses to investigate effects of exposures on the livers of *Apoe*$^{-/-}$ mice. Mice were exposed to 3R4F reference CS, to an aerosol from the Tobacco Heating System (THS) 2.2, a candidate modified risk tobacco product (MRTP) or to filtered air (Sham) for up to 8 months. THS2.2 takes advantage of a "heat-not-burn" technology that, by heating tobacco, avoids pyrogenesis and pyrosynthesis. After CS exposure for 2 months, some groups were either switched to the MRTP or filtered air. While no group showed clear signs of hepatotoxicity, integrative analysis of proteomics and transcriptomics data showed a CS-dependent impairment of specific biological networks. These networks included lipid and xenobiotic metabolism and iron homeostasis that likely contributed synergistically to exacerbating oxidative stress. In contrast, most proteomic and transcriptomic changes were lower in mice exposed to THS2.2 and in the cessation and switching groups compared to the CS group. Our findings elucidate the complex biological responses of the liver to CS exposure. Furthermore, they provide evidence that THS2.2 aerosol has reduced biological effects, as compared with CS, on the livers of *Apoe*$^{-/-}$ mice.

Keywords

Data integration, inhalation toxicology, lipidomics, modified risk tobacco product, quantitative proteomics, reduced risk product, systems toxicology, transcriptomics

History

Received 11 December 2015
Revised 14 January 2016
Accepted 1 February 2016
Published online 23 March 2016

Downloaded by [PMP S A], [Bjoern Titz] at 08:38 28 April 2016

Introduction

Cigarette smoke (CS) contains many compounds that exert biological effects, increasing the risk of cardiovascular and pulmonary diseases as well as carcinogenesis in exposed individuals. Though smoking *per se* does not appear to cause liver injury in healthy people, a growing body of evidence suggests that CS may impact incidence, severity and clinical course of chronic liver diseases (Whitehead et al., 1996). Indeed, in adult smokers with chronic liver diseases such as primary biliary cirrhosis and chronic hepatitis C, an increased severity of hepatic fibrosis has been well established (Pessione et al., 2001; Tsochatzis et al., 2009; Zein et al., 2006). Moreover, CS was identified as an independent risk factor for the onset of non-alcoholic fatty liver disease (NAFLD) (Hamabe et al., 2011) and was associated with advanced liver fibrosis in a large multi-center cohort of NAFLD patients (Zein et al., 2011).

Possibly contributing to the hepatic effects mentioned above, CS constituents can induce several liver xenobiotic-metabolizing enzymes. These include cytochrome P450 enzymes and glutathione S-transferases, enzymes whose genetic polymorphisms have, in turn, been associated with a higher risk of CS-related diseases (Daly et al., 1994; Hayes et al., 2005; Smith & Harrison, 1997; Zevin & Benowitz, 1999). Xenobiotic metabolizing enzymes are powerful radical scavengers representing the last line of defense against accumulation of reactive oxygen species (ROS). Both direct and indirect mechanistic links between CS constituents, oxidative stress and hepatotoxicity have been identified. For example, the vast quantities of carbon- and oxygen-centered

*These authors contributed equally to this study.

Address for correspondence: Julia Hoeng, PhD, MBA, Philip Morris International Research and Development, Quai Jeanrenaud 5, Neuchatel, 2000, Switzerland. E-mail: Julia.hoeng@pmi.com

Downloaded by [PMP S A], [Bjoern Titz] at 08:38 28 April 2016

free radicals contained in CS directly initiated and propagated the process of lipid peroxidation in hepatic and extra-hepatic tissues (Church & Pryor, 1985; Helen & Vijayammal, 1997). Alternatively, via an indirect mechanism, CS induced abnormally high hemoglobin levels in the blood (Young & Moss, 1989), subsequently resulting in hepatic iron overload and, finally, causing increased ROS generation in the liver (Thomas et al., 2009).

Moreover, as the liver is the major site of synthesis and absorption of plasma lipids and lipoproteins, it has been suggested that CS-related liver dysfunction may contribute to the atherogenic plasma lipid profiles observed in cigarette smokers (Boué et al., 2012; De León et al., 2013; Gepner et al., 2011; U.S. Department of Health and Human Services, 2010).

To reduce smoking-related health risks – complementing the preferred approach of smoking cessation – modified risk tobacco products (MRTP) are being developed (Kogel et al., 2014; Moennikes et al., 2008; Phillips et al., 2015; Schorp et al., 2012; Terpstra et al., 2003; Werley et al., 2008). A recent candidate MRTP developed by Philip Morris International is the Tobacco Heating System (THS) 2.2, which relies on the ''heat-not-burn'' principle. An electronically regulated device heats tobacco in a controlled fashion to release nicotine and volatiles contributing to tobacco flavors while avoiding pyrogenesis and pyrosynthesis, thus reducing formation of harmful or potentially harmful constituents (HPHCs). Our previous study (Phillips et al., 2016) compared levels of 56 HPHCs produced by THS2.2 aerosol and 3R4F CS, finding that THS2.2 produced markedly less of these components.

As one component of our comprehensive systems toxicology assessment framework for THS2.2 (Sauer et al., 2015; Sturla et al., 2014), we conducted an inhalation study with Apolipoprotein E-deficient (*Apoe*$^{-/-}$) mice. In this study, *Apoe*$^{-/-}$ mice were exposed for up to 8 months to either mainstream CS from 3R4F reference cigarettes or to aerosol from THS2.2 (with nicotine concentration matched to that of the CS, at 29.9 mg/m^3). In addition, to model effects of smoking cessation and switching to the candidate MRTP, two groups of mice were first exposed to CS for 2 months, then the exposure was changed to filtered air (cessation) or to THS2.2 aerosol (switching) for up to 6 additional months (Figure 1). Our assessments of the pulmonary and cardiovascular effects of these exposures have been reported elsewhere (Phillips et al., 2016; Titz et al., 2016). Our present report is focused on the liver-related endpoints of this comprehensive assessment study.

Previously published studies have already demonstrated the suitability of the *Apoe*$^{-/-}$ mouse model to examine links between CS exposure and several smoking-related diseases, including effects on the liver (Arunachalam et al., 2010; Boué et al., 2012, 2013; De León et al., 2013; Lietz et al., 2013; Nakashima et al., 1994). Most noteworthy are two reports showing effects of smoking and smoking cessation in plasma, aortic tissue and liver (Boué et al., 2012; De León et al., 2013). In these studies, a hepatic transcriptome analysis revealed key functions, including xenobiotic metabolism and lipid biosynthesis, affected by CS exposure and smoking cessation.

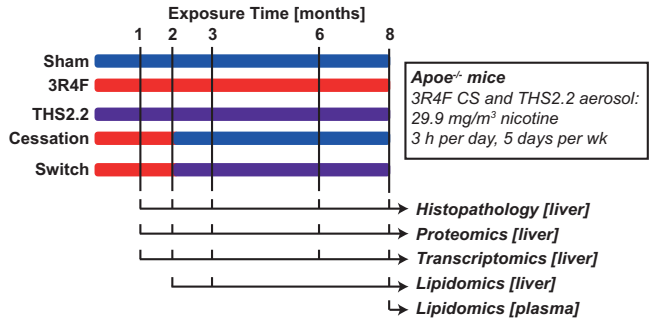


Figure 1. Experimental design and endpoints to assess effects of CS and THS2.2 exposures in livers of *Apoe*$^{-/-}$ mice. Mice were exposed to cigarette smoke (CS, 3R4F), aerosol from a candidate MRTP (THS2.2) or fresh air (Sham). Some mice were exposed to CS for 2 months and then either underwent cessation or were switched to the MRTP. The nicotine concentration was matched between CS and THS2.2 exposures (29.9 mg/m^3) and the mice were exposed for 3 h/day, for 5 days/ week. Liver tissue and plasma samples for proteomics, transcriptomics, lipidomics and histopathology were collected at the indicated time points.

Our 8-month study of THS2.2 exposure included several endpoints relevant to the liver, specifically liver tissue histopathology and quantitative measurements of the liver proteome, liver transcriptome and liver and plasma lipidomes. Our integrative analysis of these endpoints assessed the overall impact of the different exposure conditions on the liver. Consistent with previous reports (Whitehead et al., 1996), overt hepatotoxic effects were not detected in any of the exposure groups. However, at the molecular level, CS-exposure clearly affected several functional pathways, including inducing xenobiotic and oxidative stress response programs and modifying liver lipid metabolism. Interestingly, there was also evidence for an iron-related molecular response in the CS-exposed mice, which could be explained by the increased hemoglobin levels found in this group. In contrast, effects seen in CS-exposed mice were either absent or much reduced in mice exposed instead to THS2.2 aerosol. In addition, levels of the affected molecules in CS-exposed mice subjected to cessation or switching quickly approached those in sham-exposed mice. Therefore, this study provides evidence that exposure to THS2.2 aerosol, as compared with CS, leads to reduced biological effects in the liver of *Apoe*$^{-/-}$ mice.

Materials and methods

For more details, see Supplementary methods.

Experimental design

Data presented here on the effects of CS and THS2.2 exposures on the liver of *Apoe*$^{-/-}$ mice were obtained as part of a more comprehensive systems toxicology assessment study. We have written separate publications describing the other endpoints, including exposure effects on the respiratory system (Phillips et al., 2016; Titz et al., 2016).

Briefly, this study tested effects of CS and candidate MRTP (THS2.2) aerosol exposures, compared with control air (sham exposure), on liver tissue in female *Apoe*$^{-/-}$ mice. Five groups of mice were included: sham (exposed to fresh air), CS (exposed to mainstream smoke from 3R4F, a

Downloaded by [PMP S A], [Bjoern Titz] at 08:38 28 April 2016

reference cigarette from the University of Kentucky), MRTP (exposed to THS2.2 aerosol), smoking cessation (CS followed by fresh air) and switching to MRTP (CS followed by MRTP). Mice were exposed for up to 8 months. To model effects of smoking cessation and switching to the candidate MRTP, groups of mice were first exposed to CS for 2 months and, where indicated, exposure was changed to filtered air (cessation) or MRTP (switching) for an additional 6 months.

Liver samples for lipidomics analysis were collected after 2, 3 and 8 months exposure (Figure 1). Plasma samples for lipidomics were collected at 8-month exposure only. Liver tissue samples for histopathology, proteomics and transcriptomics analysis were collected after 1, 2, 3, 6 and 8 months exposure. Each group analyzed for lipidomics included eight mice, providing eight biological replicates.

Animals

All procedures involving animals were approved by an Institutional Animal Care and Use Committee, in compliance with the National Advisory Committee for Laboratory Animal Research (NACLAR) Guidelines on the Care and Use of Animals for Scientific Purposes. In accordance with the ''3Rs'' principles of animal research, Replacement, Reduction and Refinement, we used the minimum number of animals needed to obtain valid results and the least invasive procedures to minimize pain and distress. Moreover, our laboratory technicians and veterinary specialists are trained in the latest techniques to most effectively and humanely manage and care for animals. Female B6.129P2-*Apoe* (tm1Unc)N11 (*Apoe*$^{-/-}$) mice, bred under specific pathogen-free conditions, were from Taconic Biosciences (Germantown, NY). The mice were 8–10 weeks old at the start of exposures.

Reference cigarettes and MRTPs

Reference 3R4F cigarettes were purchased from the University of Kentucky (Lexington, KY, http://www.ca.uky.edu/refcig). THS2.2 consists of a stick containing a tobacco plug inserted into a holder that electronically heats the tobacco in a controlled manner, ensuring that combustion temperatures are not reached. This process generates an aerosol containing mainly water, glycerin, nicotine and tobacco flavors. THS2.2 sticks were produced by Philip Morris International (PMI; Neuchâtel, Switzerland) and cigaret holders were provided by PMI.

Smoke generation and animal exposure

Mainstream CS from 3R4F cigarettes was generated on 30-port rotary smoking machine (type PMRL-G, SM2000) as described previously (Phillips et al., 2015). Aerosols from THS2.2 sticks were generated on modified 30-port rotary smoking machines equipped with the appropriate holders. Two modified smoking machines per whole body exposure chamber were required to achieve the target THS2.2 nicotine concentration (29.9 mg/m^3). 3R4F cigarettes and THS2.2 sticks were smoked according to the Health Canada Intensive Smoking Protocol based on ISO standard 3308 (revised in 2000), with the exception of the puff volume (55 ml) and puff frequency (one puff every 30 s), as described previously (Phillips et al., 2015). Several additional minor deviations from ISO standard 3308 were necessary for technical reasons (Phillips et al., 2015). Aerosols were further diluted with conditioned fresh air to achieve the target concentrations.

The *Apoe*$^{-/-}$ mice were whole body-exposed to diluted mainstream smoke from 3R4F (600 mg TPM/m^3 corresponding to 29.9 mg/m^3), THS2.2 mainstream aerosol (nicotine-matched to 3R4F 29.9 mg/m^3) or filtered air for 3 h/day, 5 days/week, for up to 8 months. Mice received intermittent daily exposure to fresh filtered air for 30 min after the first hour of smoke exposure and for 60 min after the second hour of exposure. This was done to avoid accumulation of excessive carboxyhemoglobin (COHb) in the 3R4F group. For the sham group, mice were exposed to only filtered fresh air. Reproducibility of smoke generation and uptake was ensured by periodic analysis of the test atmosphere and measurement of biomarkers of exposure (e.g. COHb, nicotine and cotinine levels; Table 1). For the complete analyses, results and the specific methods the reader is referred to Phillips et al. (2016).

Histopathology

Histological processing was performed by Philip Morris International Research Laboratories Pte Ltd, Singapore and digitalized histological slide images were sent to Histovia (Histovia GmbH, Overath, Germany) for morphometric and histopathological evaluations.

In addition to evaluating H&E-stained sections, the fat content within hepatocytes was estimated on frozen tissue sections stained with Oil Red. The amount of glycogen within hepatocytes was estimated on sections stained with a combination of PAS and PAS-D (absence of PAS staining after enzymatic digestion of glycogen). Semi-quantitative histopathological evaluation and quantitative liver morphometry were carried out by a board-certified veterinary pathologist in a blinded fashion (Histovia GmbH, Overath, Germany). Upon completion of the evaluation, animal numbers were decoded and the unblinded data from the study groups were subjected to statistical analysis using the Cochran–Mantel–Haenszel

Table 1. Biomarkers of exposure at the 8-month time point.

		Sham	3R4F	THS2.2	Cessation	Switch
Blood	Nicotine (ng/ml)	2.7 ± 1.2	109.5 ± 12.1	118.7 ± 12.4	4.0 ± 2.0	102.7 ± 19.5
	Cotinine (ng/ml)	0.9 ± 0.3	286.5 ± 35.0	364.0 ± 50.0	0.8 ± 0.2	248.6 ± 26.5
	COHb (%)	5.4 ± 0.1	33.4 ± 2.0	6.0 ± 0.1	5.2 ± 0.1	6.6 ± 0.1
Urine	Total nicotine metabolites (μmol/l)	1.4 ± 0.1	287.6 ± 44.6	284.1 ± 50.8	1.8 ± 0.2	206.2 ± 32.3

Nicotine and cotinine measured in blood, total nicotine metabolites and carboxyhemoglobin (COHb) measurements are shown here (mean concentration ± SEM). For more details, additional biomarkers of exposure, and other time points, please refer to (Phillips et al., 2016).

Downloaded by [PMP S A], [Bjoern Titz] at 08:38 28 April 2016

test. The following semi-quantitative severity grading (1–5) was applied for all blinded histopathological endpoints: score 0: equal to the morphology of untreated animals; score 1: minimal alteration; score 2: minimal to moderate alteration; score 3: moderate alteration; score 4: moderate to severe alteration; and score 5: severe alteration.

Proteomics analysis

Our general quantitative proteomics approach was previously described (Phillips et al., 2015; Titz et al., 2014) (see Supplementary methods for details). Briefly, samples were homogenized in tissue lysis buffer (BioRad, Hercules, CA), and proteins were precipitated. Aliquots of the precipitated samples, each containing 50 µg protein, were subjected to further analysis. These samples were processed using TMT 6-plex labeling (Thermo Scientific, Waltham, MA) according to the manufacturer's instructions. Samples were analyzed using liquid chromatography coupled (Easy-nanoLC™ 1000) with tandem mass spectrometry (Q-Exactive MS mass-analyzer) (Thermo Scientific, Bremen, Germany). Data were normalized, quantified and statistically compared to identify differentially abundant proteins in the R environment (see Supplementary methods). The Benjamini–Hochberg FDR multiple test correction was employed and proteins with an adjusted $p < 0.05$ were considered to be differentially expressed.

Transcriptomics analysis

Total RNA was isolated from tissues using the miRNeasy Mini Kit (Qiagen, Hilden, Germany) and quality checked using the Agilent 2100 Bioanalyzer (Agilent Technologies, Santa Clara, CA). Total RNA (100 ng) was reverse-transcribed, amplified, purified and hybridized on MG430 2.0 GeneChips (Affymetrix, Santa Clara, CA) and evaluated using standard procedures (for details, see Supplementary methods). Raw data (CEL) files were processed with custom computable document format files from BrainArray and normalized using fRMA (McCall et al., 2010). Following quality control procedures, raw p values were generated for contrasts between control and treatments with the limma package (Ritchie et al., 2015), and adjusted using the Benjamini–Hochberg false discovery rate (FDR) multiple test correction (Gentleman et al., 2004).

Lipidomics analysis

Molecular lipids from liver tissue and plasma were extracted and quantified by Zora Biosciences (Espoo, Finland) according to internal Standard Operating Procedures, Lab Method Sheets and data Processing Method Sheets (Boué et al., 2012; Jung et al., 2011). Specific details are given in the Supplementary methods. Lipid levels were normalized to their respective internal standards and the sample volume or tissue weight. Concentrations of molecular lipids are presented as nmol/mg wet tissue. For differential abundance analyses, only those lipid species that were present in at least 50% of the samples of each of the compared groups were included. The Benjamini–Hochberg FDR multiple test correction was employed at the contrast level for t-test derived p values and lipid species with an adjusted $p < 0.05$ were considered to be differentially abundant.

Additional data analysis methods

Protein set analysis was supported by the Piano package in the R statistical environment (Väremo et al., 2013). Pathway maps were obtained from the KEGG database (Kanehisa et al., 2014). Set enrichment was assessed by over-representation analysis (ORA) and gene-set analysis (GSA). A one-tailed Fisher's exact test was employed for ORA. For GSA, we used the fold-change compared with sham exposure as the protein-level statistic, the mean as the set statistic and sample permutation (Q2) to assess statistical significance. p Value adjustment was done with the Benjamini–Hochberg procedure. The sparse partial least squares (sPLS) approach was conducted in the canonical mode with the mixOmics package in R (Lê Cao et al., 2009). Functional associations among proteins were obtained from the STRING database (Szklarczyk et al., 2015). Functional clusters were manually annotated guided by ToppGene (Chen et al., 2009).

Data availability

The mass spectrometry proteomics data are available from the ProteomeXchange Consortium via the PRIDE partner repository (http://www.ebi.ac.uk/pride/archive/) (Vizcaíno et al., 2014). The database identifier is PXD002925. The lipidomics data are available in the supplement (Supplemental Table S2). The transcriptomics data have been submitted to ArrayExpress with the identifier E-MTAB-3876.

Results

A comprehensive systems toxicology study on *Apoe*$^{-/-}$ mice was conducted to assess effects of THS 2.2, compared with reference cigarettes (3R4F), focusing on cardiovascular and pulmonary endpoints (Phillips et al., 2016). The study design is summarized in Figure 1. In order to verify the reproducibility of smoke/aerosol uptake, a number of biomarkers were measured and summarized in Table 1 [for more details please refer to Phillips et al. (2016)]. Here, we present results of liver transcriptomics, proteomics, lipidomics and histopathology including plasma lipidomics obtained with samples from the same study.

Time-dependent liver changes were consistent with age-dependent changes in the *Apoe*$^{-/-}$ genotype

The specific genotypic and phenotypic features of *Apoe*$^{-/-}$ mice make them the most widely used preclinical model for atherosclerosis (Zhang et al., 1992). In fact, *Apoe*$^{-/-}$ mice show delayed lipoprotein clearance and consequently develop hyper- and dyslipoproteinemia, severe hypercholesterolemia and atherosclerotic lesions even when on a normal diet (Nakashima et al., 1994). Recently, De León et al. (2013) reported on effects of smoking cessation on hepatic lipid and transcriptomics profile in *Apoe*$^{-/-}$ mice, confirming the suitability of the model for studying CS effects on liver physiology.

In our study, principal component analysis (PCA) of the liver transcriptome data clearly separated the samples of

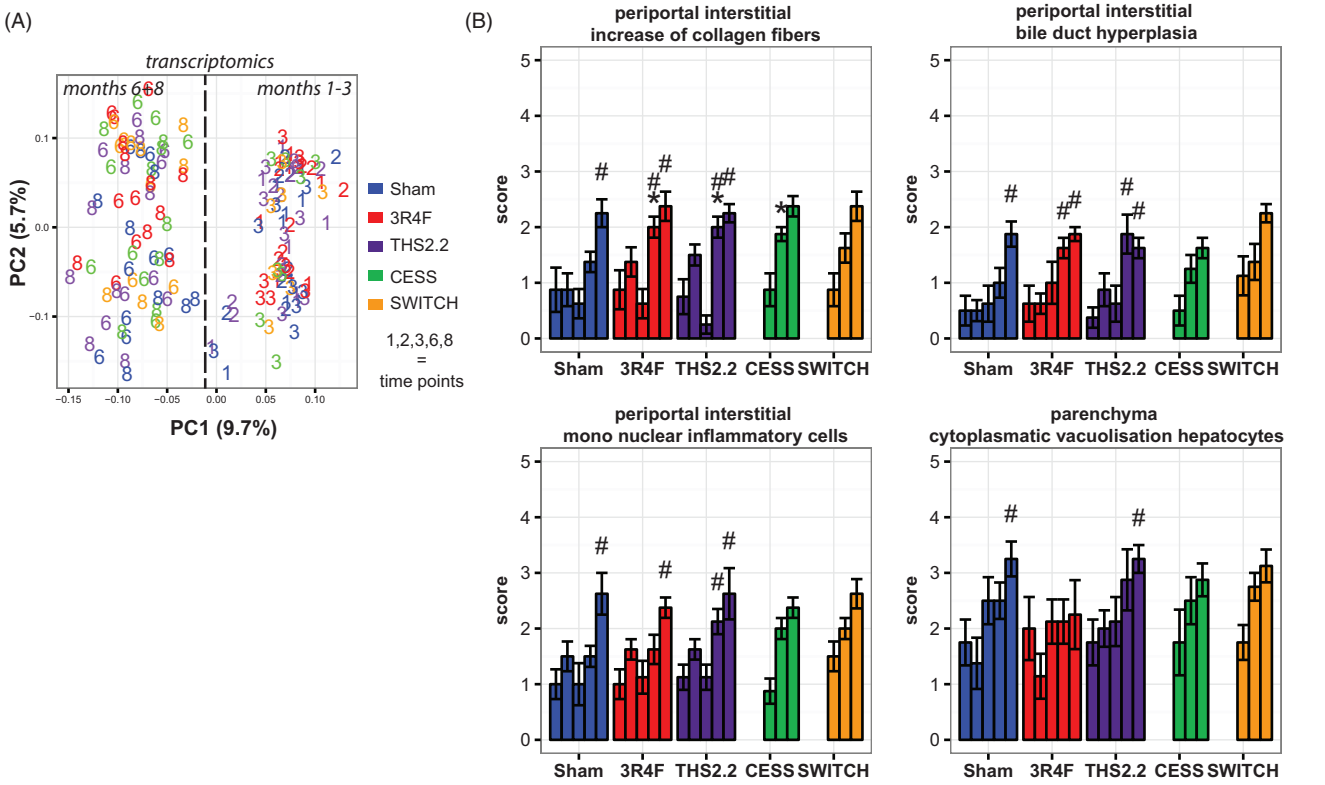


Figure 2. *Apoe*$^{-/-}$ mice demonstrated time-dependent, though mostly exposure group-independent, changes in the liver during the 8-month exposure period. (A) Principal component analysis (PCA) of transcriptomics data showing clear separation between early (months 1–3) and late (months 6 and 8) time points. PCA score plot for component 1 (PC1, 9.7% explained variance) and component 2 (PC2, 5.7% explained variance). The numbers represent exposure duration and the colors represent exposure groups of the samples (see color key). Note that PC1 separates the early (months 1–3) from late (months 6 and 8) time points, whereas a clear separation of exposure conditions is not apparent. (B) Four selected histopathology endpoints showing significant changes over time. Data are means ± SEM, $n = 8$. Statistics: *$p < 0.05$ compared with sham at same time point; #$p < 0.05$ compared with month 1 for the same exposure group. See Supplemental Figure S1 for all liver histopathology endpoints.

Downloaded by [PMP S A], [Bjoern Titz] at 08:38 28 April 2016

the early (months 1–3) and later (months 6 and 8) time points, but did not separate the different exposure groups (Figure 2A). To evaluate whether this time dependent trend in the data was consistent with known changes in Apoe-deficient mice, we conducted a gene-set enrichment analysis (GSEA) for the transcripts that contributed to the separation between early and later time points. Liver transcripts positively associated with the later time points (months 6 and 8) were significantly enriched for gene sets associated with oxidative phosphorylation, aging, inflammation, cholesterol and nicotinate metabolism and interferon gamma signaling (Supplemental Table S1). Interestingly, these pathways are known to be involved in age-related liver dysfunction and CS-associated processes (Bonomini et al., 2013; El-Zayadi, 2006; Sheedfar et al., 2013). In addition, histopathology confirmed that the livers of *Apoe*$^{-/-}$ mice developed several significant changes over time – again with the largest differences between the early (months 1–3) and later (months 6 and 8) time points (Figure 2B). Indeed, accumulation of collagen fibers, as well as parenchymal vacuolization, degeneration and necrosis, periportal and interstitial mononuclear inflammatory cells and bile duct hyperplasia, were significantly greater at later time points, more so than any differences among the exposure groups. Taken together these results showed the expected time-dependent evolution of both molecular and histological end points in the livers of *Apoe*$^{-/-}$ mice. Having established these time-dependent changes, we next analyzed exposure-dependent effects within each time point.

Absence of overt hepatotoxicity by CS and THS2.2 exposures in *Apoe*$^{-/-}$ mice

Chemicals yielded by CS induce both direct and indirect effects. For example, CS components directly induce oxidative stress associated with lipid peroxidation and inflammation, increasing the incidence, severity and clinical course of many chronic liver diseases (Pessione et al., 2001; Yu et al., 1997).

To identify potential hepatotoxic effects of CS or THS2.2 exposures, a panel of marker proteins and genes for liver toxicity was evaluated (Figure 3A and B) (Koturbash et al., 2011). Of this panel, only 1 gene (Cyp1a2) of 99 and only a few proteins demonstrated statistically significant exposure-associated changes. In this regard, our molecular analysis did not provide evidence for overt hepatotoxicity in any of the exposure groups. However, there were significant and directionally consistent changes in expression of Cd36, lanosterol synthase (Lss), flavin containing monooxygenase 1 (Fmo1) and carbonic anhydrases (Car3) and strong upregulation of Cyp1a2 in

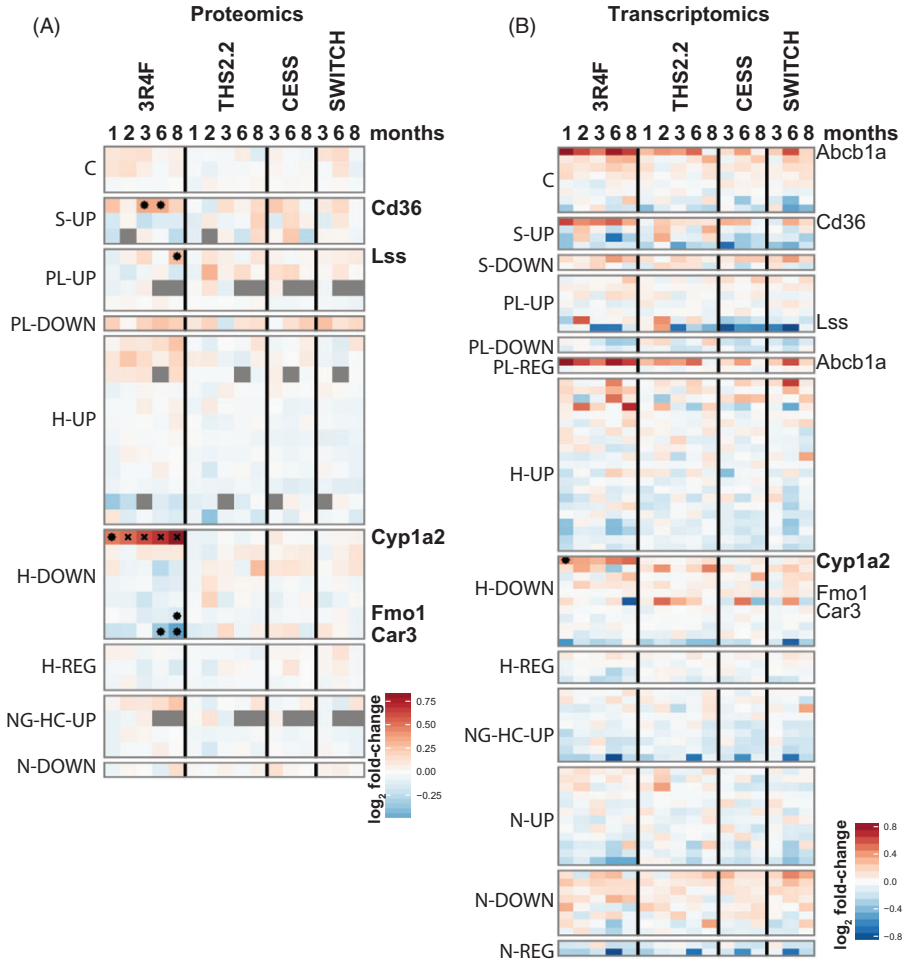


Figure 3. Exposed mice did not show signs of overt hepatotoxicity. Hepatotoxicity marker response profiles for the different exposure groups and the proteomics (A) and transcriptomics (B) data. Expression response profiles for a list of curated hepatotoxicity markers (SA Biosciences, Madison, WI) are shown. The fold-changes are color-coded and statistically significant differences are marked (Benjamini–Hochberg (BH)-adjusted *p*-value, * ≤ 0.05, *x* ≤ 0.01). Missing values are gray. C = cholestasis, S-UP/DOWN = steatosis (up, down), PL-UP/DOWN = phospholipidosis (up/down), H-UP/DOWN/REG = hepatotoxicity (up, down, regulated), NG-HC-UP/DOWN = nongenotoxic hepatocarcinogenicity (up/down), N-UP/DOWN = necrosis (up/down).

Downloaded by [PMP S A], [Bjoern Titz] at 08:38 28 April 2016

the liver proteomes of CS-exposed mice. This suggested that CS exposure induced several molecular effects in the liver, as discussed in more detail below.

In addition, histopathological analysis of the liver tissue was conducted to assess possible hepatotoxic-related microscopic features (Figure 2B and Supplemental Figure S1). Overall, in accordance with the results of molecular analysis, there were no clear time-consistent differences in histopathology endpoints among the exposure groups. For example, cytoplasmic vacuolization, periportal interstitial bile duct hyperplasia and periportal interstitial mono nuclear inflammatory cells showed an increase over time in all groups, probably due to the changes that normally occur with age in *Apoe*$^{-/-}$ mice, but there were no significant differences among exposure groups. The only exception was after 6 months, when a more pronounced increase in periportal interstitial collagen fibers was observed for the 3R4F, THS2.2 and cessation groups compared with the sham group. However, the difference among exposure groups was minimal compared with the age-related increases in collagen fibers.

Taken together, analysis of the transcriptome and proteome, along with histopathology, provided no clear indications of CS or THS2.2 exposure-induced hepatotoxicity. These observations agreed with reported CS-related effects in humans, that is, that CS exposure alone was not associated with overt hepatotoxicity or chronic liver disease (Whitehead et al., 1996).

Integrative analysis of liver transcriptome and proteome revealed CS-specific exposure effects

Next, we assessed whether a more extensive analysis of molecular changes could reveal biologically relevant exposure effects. Importantly, some proteins and genes did show statistically significant differential expression in the 3R4F-exposed, compared with sham-exposed, group (Figure 4A and B). However, the number of differentially expressed genes was low and the first PCA components from the transcriptomics data indicated only the above-mentioned separation by exposure times (Figure 2A and Supplemental Figure S2A). In addition, the first PCA components for the proteomics data did not show a separation of the samples either by time or by exposure conditions (Supplemental Figure S2B). We therefore investigated whether an integrative analysis of exposure effects on the proteome and the transcriptome would more clearly reveal molecular exposure effects, applying the multivariate canonical sPLS (sPLS-can) analysis approach. Conceptually, sPLS-can is related to PCA; however, rather than identifying the major new data components that best explain the variance of individual datasets, sPLS-can identifies those new components in the data that best correlate

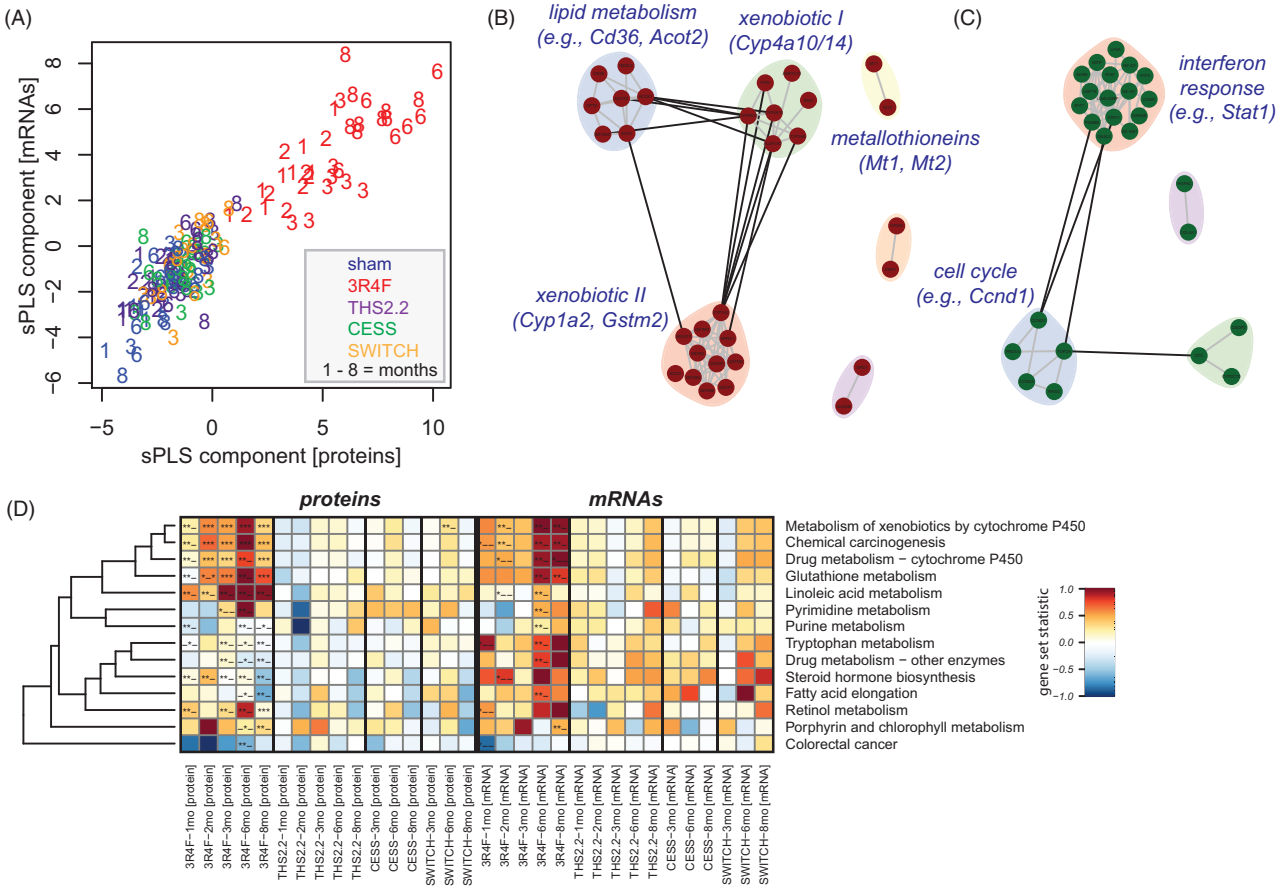


Figure 4. CS exposure induced a molecular response in the liver. (A) Identification of a shared component by sparse PLS-can between the proteomics and transcriptomics data showing separation of the exposure groups. Transcriptomics and proteomics data for liver samples were integrated using sparse PLS-can to identify the major shared trends among the data types. The identified component with the largest correlation separated the exposure groups (component 3 in Supplemental Figure S2). Exposure groups are color-coded and the numbers indicate the time point in months. (B) Clustered functional association network for proteins/genes with positive contributions to the correlated component (i.e. with an upregulation trend in the 3R4F groups). The identified clusters were manually annotated guided by ToppGene (Chen et al, 2009). (C) As in B, but for genes/proteins with negative contributions to the identified component (i.e. with a downregulation trend in the 3R4F groups). (D) Protein and gene set enrichment analysis. Set enrichment was assessed by over-representation analysis (ORA) and gene-set analysis (GSA). For GSA, the fold-change compared with sham exposure was used as the protein-level statistic, the mean as the set statistic and sample permutation (Q2) to assess statistical significance. Enrichment results are normalized per pathway. Significant differences are indicated by asterisks (*BH-adjusted p-value < 0.05). The first asterisk represents the overall adjusted Fisher p-value of the GSA and ORA analyses, the second asterisk the GSA and the third asterisk the ORA results. Significantly affected pathways (BH-adjusted p-value < 0.05) in any of the comparisons of both proteomics and transcriptomics data are shown. See Supplemental Figure S3 for all significantly changed gene/protein sets, including the sets that were only significant for one of the data modalities.

between two datasets (Figure 4A and Supplemental Figure S2C). The identified component with the highest correlation between the mRNA and protein data indicated a clear separation between CS-exposed mice and those in the other groups, while also highlighting a time-dependent trend with increased scores for the later time points. To understand which molecules were driving this separation, a functional clustering approach was applied (Figure 4B and C). This analysis showed that lipid metabolism and xenobiotic phase 1 and 2 proteins/genes tended to be more highly expressed in CS-exposed mice than in other groups (i.e. they showed a positive association with CS-exposed samples) (Figure 4B). Conversely, interferon gamma response and cell cycle proteins/genes tended to be downregulated in CS-exposed groups relative to the other groups (Figure 4C).

We complemented these results with a gene-set analysis (GSA), in which we focused on gene-sets that were significantly affected in both the proteome and the transcriptome (Figure 4D and Supplemental Figure S3). Most prominent among the shared gene-sets were xenobiotic and lipid metabolism-related functions, confirming the sPLS-can observations (Figure 4A, D, and Supplemental Figure S3). Interestingly, GSA also highlighted CS-dependent activation of a specific gene-set, ‘‘Porphyrin and chlorophyll metabolism’’ that mainly contains genes and proteins implicated in iron metabolism. This observation might be related to the presence of metallothioneins 1 and 2 among the clusters of genes with increased expression in the CS-exposed group (Figure 4B) and led to further analysis of the potential role of iron metabolism, described in more detail below. Overall, the results of our analyses suggested a CS-specific effect on well-characterized molecular pathways in the liver involving lipid, xenobiotic and possibly iron metabolism. These data were, overall, consistent between mRNA and protein profiles. The data also indicated an absence of THS2.2-related effects and the tendency for the CS-associated effects to be reversed

Downloaded by [PMP S A], [Bjoern Titz] at 08:38 28 April 2016

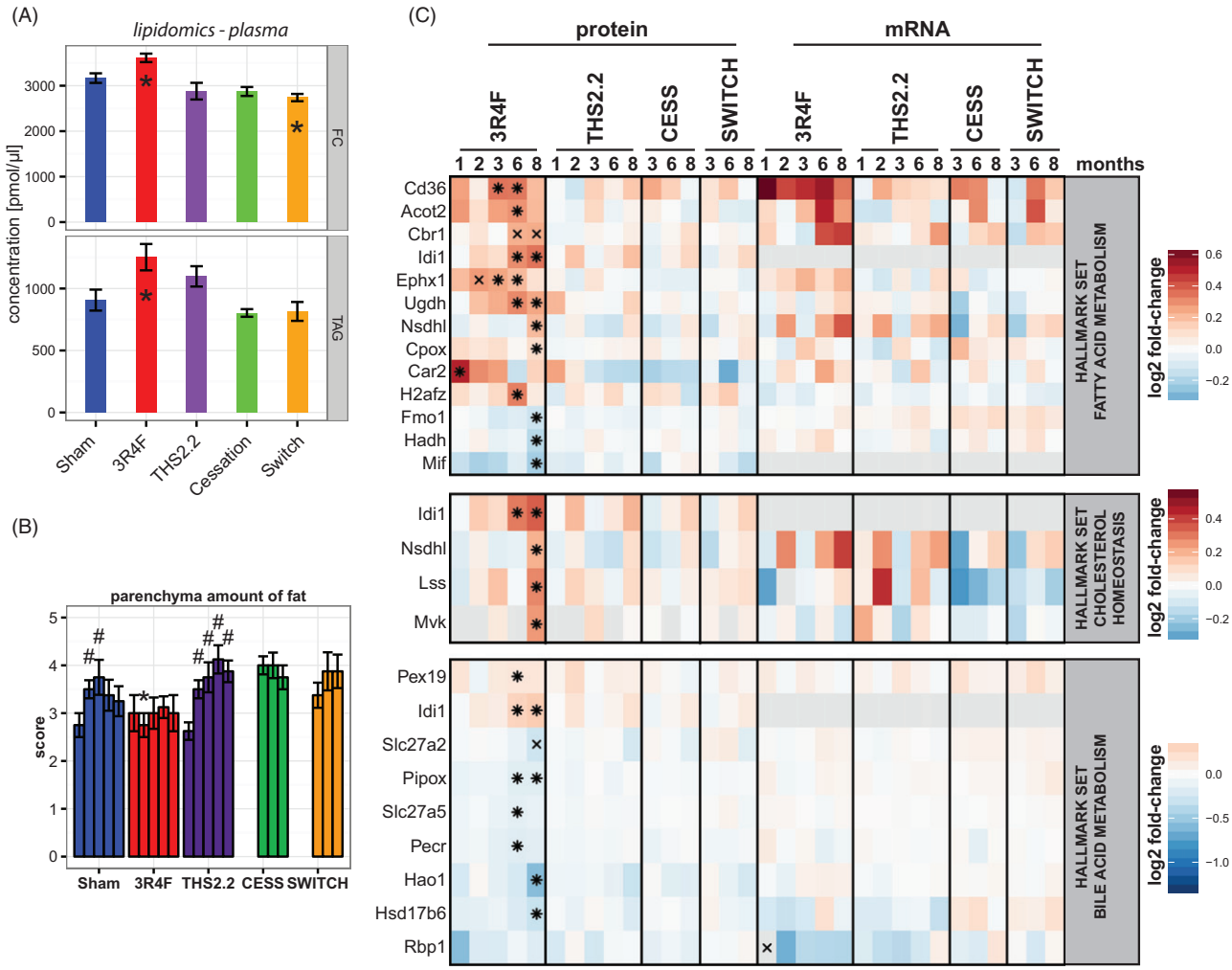


Figure 5. CS exposure affected lipid metabolism in *Apoe*$^{-/-}$ mice. (A) Significantly affected lipid classes in plasma after 8 months exposure. The mean concentrations ± SEM are shown. *p < 0.05 (compared with Sham group). See Supplemental Figure S4 for the non-significant lipid classes and for results at the level of individual lipid species. (B) Histopathology endpoint: amount of fat in liver parenchyma. Data are means ± SEM, $n = 8$. Statistics: *$p < 0.05$ compared with sham at same time point; #$p < 0.05$ compared with 1 month within same exposure group. See Supplemental Figure S1 for all liver histopathology endpoints. (C) Protein and gene expression profiles for three lipid-metabolism related panels. Profiles for significantly affected proteins or genes (BH-adjusted p-value < 0.05) of three hallmark gene/protein sets are shown: fatty acid metabolism, cholesterol homeostasis and bile acid metabolism (www.broadinstitute.org/gsea/msigdb) (Liberzon et al., 2011). The fold-changes compared with the respective sham groups are color-coded and statistically significant differences are marked (BH-adjusted p-value, * ≤ 0.05, x ≤ 0.01). Missing values are gray.

upon cessation and switching to THS2.2. The implications of the response of these three specific pathways to CS and their potential inter-connections were discussed as follows.

Cigarette smoke induced changes in liver and plasma lipid metabolism

Previous reports showed a smoking-dependent trend toward increased lipid levels in the liver and plasma (Boué et al., 2012; De León et al., 2013; Lietz et al., 2013). This trend was partially confirmed in our study with the exception of effects on plasma free cholesterol and triglyceride levels (refer the ''Discussion'' section). Thus, plasma lipids at 8 months showed elevated free cholesterol and triglycerides with CS exposure, as assessed through clinical chemistry by Phillips et al. (2016) and confirmed by lipidomics analysis (Figure 5A and Supplemental Figure S4). The THS2.2 group showed a lipid profile similar to that of the sham group. The cessation and switch groups no longer showed a profile significantly different from that of the sham group after the CS exposure had been interrupted (Phillips et al., 2016). Of note, total triacylglycerols (TAGs) in the plasma lipidome showed a trend toward an increase in the THS2.2 group (Figure 5A). However, this effect was not statistically significant and likely an outlier effect, that is, caused by a very high concentration of TAG 52:3 and 52:2, two of the most abundant species, in a single mouse from the THS2.2 exposed group (mouse #921024, Supplemental Figure S4C).

The liver lipidomics data showed very high intra-group variability, especially in the sham group, making the interpretation of the results challenging. Supplemental Figure S5 shows a heatmap representing levels of lipid species detected in the various exposure groups compared with those in the sham group. A few classes of ceramide (Cer d18:0, Cer d18:1, LacCer) were significantly lower in the THS2.2, switch and cessation groups at later time points. The different glycerophospholipids subclasses showed fluctuating trends. LPE

Downloaded by [PMP S A], [Bjoern Titz] at 08:38 28 April 2016

Downloaded by [PMP S A], [Bjoern Titz] at 08:38 28 April 2016

(lysophosphatidylethanolamine), PA (phosphatidic acid) and PG (phosphatidylglycerol) showed trends toward being elevated in the 3R4F-exposed group but trends toward being decreased in the THS2.2, cessation and switching groups. Of these, only the cessation and switching groups showed any statistically significant effects.

Phosphatidylcholine (PC) abundance was generally higher than sham values in all the other groups, reaching statistical significance only in the cessation group, while LysoPC (LPC) showed a trend toward being decreased in all exposure groups, relative to the sham. Finally, diacylglycerols and TAGs showed dissimilar trends. Whereas diacylglycerols showed trends toward decreasing over time, TAGs showed significant decreases in the 3R4F and THS2.2 groups, compared with sham, at early time points but a trend toward increasing over time (Boué et al., 2012; De León et al., 2013). Several TAG species could not be detected in the switch group and, at later time points, in the other groups. This makes it difficult to speculate about any impact of CS exposure on liver triacylglycerol accumulation (Supplemental Figure S5). Overall, our results indicate that, in the absence of chronic liver disease, CS exposure does not profoundly affect the liver lipidome. Our histopathological observations relevant to fat metabolism further confirmed this interpretation (Figure 5B). Despite the time-dependent increase of parenchyma fat accumulation in the liver tissue observed in all groups, no statistically significant histopathological differences among exposure groups were observed.

However, our integrative proteomics/transcriptomics analysis demonstrated a higher sensitivity for detection of possible lipid-metabolism related exposure effects. As already mentioned, a lipid metabolism protein/gene cluster contributed to the separation between the 3R4F-exposed and other groups (Figure 4A and B). To follow-up on this result, we more specifically analyzed the response of molecules in the three lipid-related hallmark gene sets from the mSigDB database: fatty acid (FA) metabolism, cholesterol homeostasis, and bile acid metabolism (Mootha et al., 2003; Subramanian et al., 2005) (Figure 5C).

Based on changes in liver protein abundances and supported by similar trends in gene expression, CS exposure affected all three hallmark sets. The abundance of several proteins in these three sets was significantly affected in the 3R4F group, with no significant changes relative to sham values in the other exposure groups. In particular, upregulation of CD36 and ACOT2 (acyl-CoA thioesterases 2) in the 3R4F group suggested the possibility of increased FA uptake and intracellular acyl-CoA and free FA levels, while hydroxyacyl-CoA dehydrogenase (Hadh) downregulation likely reflected a reduced FA oxidation potential (Figure 5C). Overall, these changes in protein abundance are consistent with the time-dependent trend toward increased TAGs observed in the liver of the 3R4F group (Supplemental Figure S5). In addition, some proteins in the hallmark set of FA metabolism are important components of the xenobiotic elimination pathways (Cbr1, Ephx1, Fmo1) (Figure 5C) (Hassett et al., 1994; Oppermann, 2007; Phillips et al., 1995). This overlap suggested functional links among the different categories affected by CS exposure in this study, as further discussed below.

The cholesterol synthesis pathway was affected in the 3R4F group at later time points. Several enzymes involved in cholesterol biosynthesis, such as isopentenyl-diphosphate delta isomerase 1(Idi1), NAD(P)H steroid dehydrogenase-like (Nsdhl), lanosterol synthase (Lss) and mevalonate kinase enzyme (Mvk) (Russell, 1992), were upregulated. These findings might contribute to the observed trend of increased liver cholesterol esters (Supplemental Figure S5) and plasma free cholesterol.

Finally, several proteins belonging to the hallmark set of bile acid metabolism showed significant changes (Figure 5C) in the livers of 3R4F-exposed mice, compared with those in other groups. The majority of these regulated proteins were peroxisomal enzymes (Ferdinandusse & Houten, 2006) showing decreased abundance, including pipecolic acid oxidase (Pipox), peroxisomal trans-2-enoyl-CoA reductase (Pecr), hydroxyacid oxidase 1 (Hao1) and hydroxysteroid (17-beta) dehydrogenase 6 (Hsd17b6). Moreover, two solute carrier family proteins (Slc) – Slc27a2 and Slc27a5 – were significantly downregulated in the 3R4F group. Slc27a2 is involved in both bile and FA metabolism and is localized in peroxisomal membranes and Slc27a5 activates the secondary bile acids entering the liver from the enterohepatic circulation. Overall, this CS-dependent downregulation of bile acid synthesis and catabolism pathways may contribute to the reported increases and accumulation of cholesterol (Boué et al., 2012; De León et al., 2013; Phillips et al., 2016). Of note, peroxisomal biogenesis factor 19 (Pex19), which is required for early stage peroxisome biogenesis, was increased, suggesting a CS-dependent effect also on other processes in which peroxisomes are critical (e.g. ROS generation; refer the ‘‘Discussion’’ section).

Taken together, transcriptome and proteome analysis showed dysregulation of liver lipid metabolism pathways in CS-exposed mice, confirming previous findings (Boué et al., 2012; De León et al., 2013; Latha et al., 1988). In particular, while enzymes involved in FA and cholesterol metabolism were consistently upregulated, those involved in bile acid synthesis and transformation were downregulated by CS exposure. In contrast, THS2.2 exposure showed reduced effects on lipid metabolism pathways in the liver. Furthermore, in the cessation and switch groups, there was a rapid loss of detectable CS-induced effects on these pathways.

Cigarette smoke-dependent induction of liver xenobiotic enzymes

Hepatic enzymes involved in phases I and II xenobiotic metabolism play central roles in the overall metabolism and disposition of endogenous and exogenous substrates. CS constituents induce several xenobiotic-metabolizing enzymes in both hepatic and extrahepatic tissues (Pavek & Dvorak, 2008; Zevin & Benowitz, 1999). As we described, expression of xenobiotic metabolism genes/proteins contributed to the separation of the 3R4F groups from the other exposure groups (Figure 4).

To gain further insights into this differential effect on xenobiotic metabolism, we evaluated exposure effects for a comprehensive panel of xenobiotic proteins/genes (Figure 6).

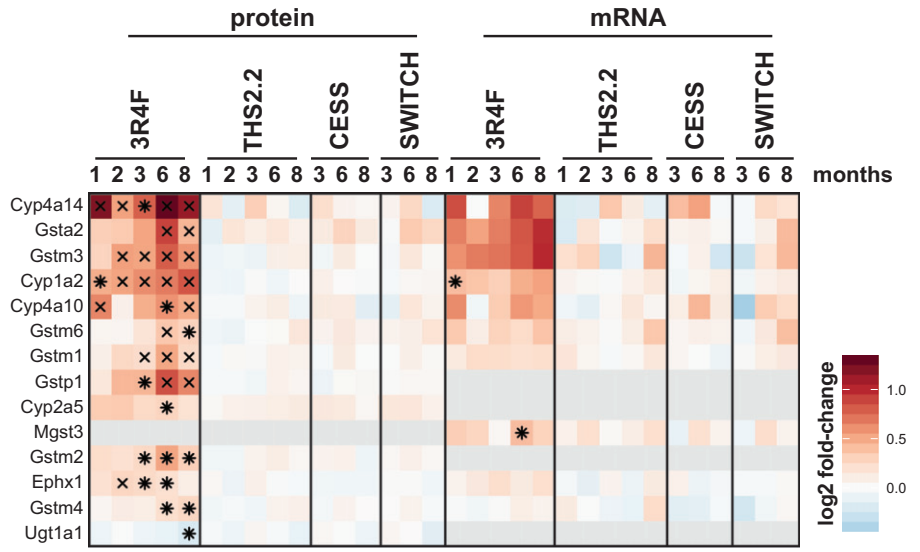


Figure 6. CS exposure induced a xenobiotic/oxidative stress response in the liver of *Apoe*$^{-/-}$ mice. Profiles for significantly affected xenobiotic/oxidative stress proteins/genes are shown (BH-adjusted $p < 0.05$). Protein/genes identified by functional clustering (Figure 4D) and extended by the metabolism of xenobiotics by cytochrome P450 pathway from the KEGG database are included (Kanehisa et al., 2014). The fold-changes compared with the respective sham groups are color-coded and statistically significant differences are marked (BH-adjusted p-value, $* \leq 0.05$, $x \leq 0.01$). Missing values are gray.

Downloaded by [PMP S A], [Bjoern Titz] at 08:38 28 April 2016

Several of these proteins were significantly upregulated upon CS exposure. The abundances of phase I (CYPs) and phase II (GSTs, UGTs) enzymes were increased, with CYPs showing effects at even the earlier time points. Among the affected CYPs were Cyp4a14 and Cyp4a10, well known PPARα target genes that catalyze oxidation of a wide variety of substrates (Hsu et al., 2007). Cyp1a2 and Cyp2a5, other enzymes regulated by CS exposure, are both expressed in the liver and responsible for metabolizing cotinine and nicotine as well as dietary and CS-derived procarcinogens such as aromatic and heterocyclic amines (Bartsch et al., 2000; Zhou et al., 2010). Finally, a number of glutathione S-transferase (GSTs) enzymes showed increased abundance in the 3R4F group, relative to the sham group. GSTs catalyze conjugation of reduced glutathione (GSH) to xenobiotic substrates resulting in detoxification and alleviation of oxidative stress. The GST family *mu* (M), particularly affected by CS-exposure in our analysis, plays a central role in phase II detoxification of ROS (Figure 6). In contrast to the 3R4F group, the THS2.2, cessation and switching groups did not demonstrate a significantly increased abundance of these or any other xenobiotic enzymes.

These data confirmed that CS exposure activated production of enzymes involved in detoxification phase I and II processes. Strikingly, no significant impact on production of those enzymes was observed following THS2.2 exposure or after cessation or switching. While these observed effects might be partially explained by a direct substrate-dependent activation (e.g. by the induction of CYPs by PAHs and nicotine), involvement of an indirect mechanism is also possible, as discussed further below.

Differential abundance of liver iron-related proteins and potential implications for the overall response to CS exposure

As already reported by Phillips et al. (2016) (also, see ‘‘Methods’’ for details), 3R4F exposure resulted in a significantly increased hematocrit, erythrocyte counts and hemoglobin levels, while such changes were not observed with THS2.2 aerosol exposure (Figure 7A). Cessation and switching resulted in a return of these parameters to sham values within 1 month. Considering the well-known link between increased red blood cell number, heme catabolism and iron accumulation, these observations suggested a potential imbalance in iron homeostasis with 3R4F exposure (El-Zayadi, 2006). This hypothesis was corroborated by the molecular profiling results (Figure 7B). In particular, a group of proteins/genes involved in liver iron homeostasis (Hentze et al., 2004) were significantly induced in the 3R4F group. Among these were ferritin light and ferritin heavy chains, which form complexes called ferritin-nanocages where cellular iron is stored (Arosio et al., 1976; Tao et al., 2014). Metallothionein 1 and 2, though they do not bind iron (Kojima et al., 1982), are considered two important radical scavengers (Abel & de Ruiter, 1989; Thornalley & Vašák, 1985) that are upregulated in the adaptive response to liver iron overload (Brown et al., 2007). Finally, increased hemoglobin synthesis by liver erythroid cells and decreased transferrin were each implicated as a cause or consequence of increased iron levels in the liver (Ghio et al., 2008).

Effects of dietary-induced iron overload on gene and protein expression in the liver were previously described in several studies (Brown et al., 2007; Moon et al., 2012; Rodriguez et al., 2009). To investigate similarities between the CS-exposure responses that we observed and the response to dietary-induced iron overload, we identified proteins that were consistently differentially expressed in our study and in three previous iron-overload studies (Brown et al., 2007; Moon et al., 2012; Rodriguez et al., 2009) (Figure 7C). Interestingly, besides specific iron-related molecules (e.g. ferritin), most of the molecules shared between our study and the iron-overload response studies were GSTs and CYPs enzymes, known to be responsive to both xenobiotics (Figure 6) and oxidative stress (Hayes & McLellan, 1999) (Figure 7C). While the overlap in proteins/genes affected among the three iron-overload studies is limited, those involved in the response to oxidative stress have already been highlighted as a core shared component of the iron-

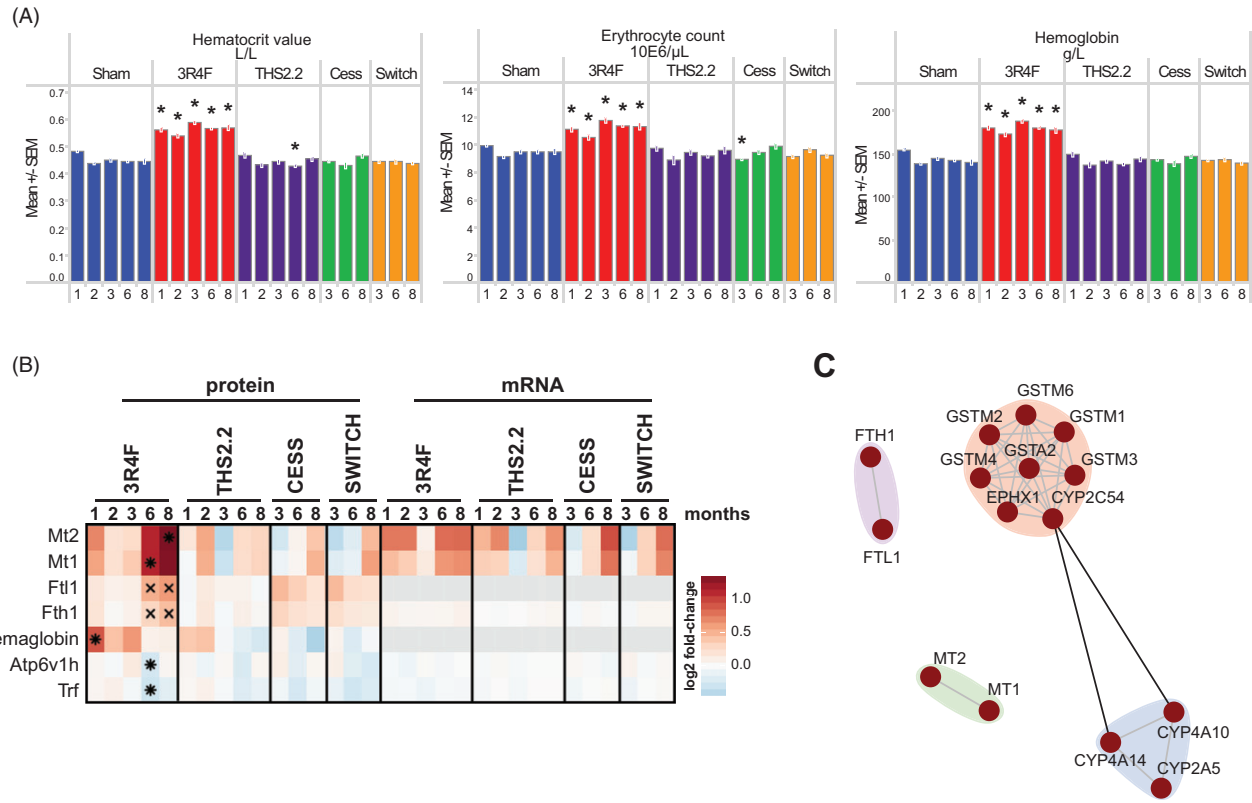


Figure 7. CS exposure results in an increased hematocrit that is associated with an iron-related protein response in liver. (A) Blood measurements of hematocrit values, erythrocyte counts and hemoglobin concentrations. The mean concentrations ± SEM are shown. *$p < 0.05$ (compared with Sham group). (B) Profiles for significantly affected iron-related proteins and genes in the liver are shown (BH-adjusted p-value < 0.05). The fold-changes compared with the respective sham groups are color-coded and statistically significant differences are marked (BH-adjusted p-value, * ≤ 0.05, $x \leq 0.01$). Missing values are gray. (C) Clustered functional association network for significantly elevated proteins/genes in this and any of three previous studies on the effect of iron-overload in mouse liver (Brown et al., 2007; Moon et al., 2012; Rodriguez et al., 2009).

overload phenotype (Brown et al., 2007; Moon et al., 2012; Rodriguez et al., 2009).

Taken together, 3R4F exposure resulted in a significantly increased hematocrit, erythrocyte counts and hemoglobin levels, which likely are also reflected by the iron-related protein expression response of the liver, supporting the idea of an iron-related activation of antioxidant defense mechanisms.

Discussion

The major goal of this study was to explore molecular events characterizing CS-induced hepatic effects and to further compare them with the less pronounced effects exerted by a newly developed candidate MRTP named THS2.2. In previous studies, we applied similar approaches (Boué et al., 2012; De León et al., 2013; Lietz et al., 2013; Phillips et al., 2015, 2016; Titz et al., 2016) to characterize modulation of plasma, aorta, lung and liver lipidomes, transcriptomes and proteomes by CS exposure and the consequences of smoking cessation in both *Apoe*$^{-/-}$ and wild-type C57B/L6 mice. For example, these studies demonstrated widespread effects of CS exposure on both the plasma and tissue lipidomes, with a clear trend toward accumulation of atherogenic lipids. Moreover, cessation improved whole body lipidomics parameters and attenuated the molecular tissue dysregulation observed with CS exposure. Importantly, effects exerted by CS exposure in the context of lipid metabolism were part of a wider response, which also included xenobiotic and oxidative stress processes.

The *Apoe*$^{-/-}$ mouse strain used in this study has been established as a useful experimental system for investigating comorbidities associated with cigarette smoking (Arunachalam et al., 2010; Boué et al., 2013; De León et al., 2013; Nakashima et al., 1994). While they show time-dependent hepatic lipid accumulation and aging-related dysfunctions (Bonomini et al., 2013) (Figure 2), *Apoe*$^{-/-}$ mice are not considered a model of chronic liver disease. This is important, because CS is not considered to cause liver disease alone, but rather aggravates pre-existing liver diseases. It will, therefore, be interesting in future studies to also test effects of CS in the context of chronic liver disease models (e.g. induced by carbon tetrachloride, dimethyl or diethyl nitrosamine or bile duct ligation) (Liu et al., 2013). However, the advantage of the *Apoe*$^{-/-}$ mouse model in this study is that it avoided possible synergistic effects that could have confounded our analysis by increasing its biological complexity. Importantly, in our study, the inclusion of extensive molecular measurements (e.g. proteomics and transcriptomics) allowed for the sensitive detection of disease onset effects of the different exposure conditions.

Thus, overall, our systems toxicology assessment study demonstrated how the broad impact of CS on different organ systems (respiratory, cardiovascular and liver) can be assessed simultaneously in a single mouse model (Phillips et al., 2016; Titz et al., 2016).

Downloaded by [PMP S A], [Bjoern Titz] at 08:38 28 April 2016

Downloaded by [PMP S A], [Bjoern Titz] at 08:38 28 April 2016

The first tier analysis in our study aimed to assess hepatotoxic effects potentially caused by CS and/or THS2.2 exposures (Figure 3 and Supplemental Figure S1). Our molecular and histopathological analyses identified no significant hepatotoxic effects intrinsically linked to CS or THS2.2 exposures. The absence of discernible hepatotoxicity was consistent with findings observed in humans. Indeed, previous clinical studies, performed to elucidate the relationship between cigarette smoke and alcohol consumption (Robinson & Whitehead, 1989; Whitehead et al., 1996), showed an alcohol dose-dependent increase of AST (aspartate aminotransferase), ALT (alanine aminotransferase) and GGT (γ-glutamyl transferase). Of these, only GTT was slightly affected by CS. These data support smoking alone not being a causative agent for liver diseases but, rather, an accelerator in the presence of synergic factors (alcohol, chronic liver diseases) (Altamirano & Bataller, 2010; Azzalini et al., 2010; Lu et al., 2013; Whitehead et al., 1996). Accordingly, proteomics and transcriptomics analyses clearly revealed molecular perturbations upon CS exposure (Figure 4 and Supplemental Figure S2) that could accelerate progression of liver diseases. In particular we observed effects on three main biological processes, lipid, xenobiotic and iron metabolism.

Previous reports (Boué et al., 2012; De León et al., 2013; Gepner et al., 2011; Lietz et al., 2013) described the extensive impact of CS on lipid homeostasis and showed that smoking cessation could reverse these effects. These studies described CS-dependent trends of elevated lipid levels in both plasma and tissues, with some exceptions such as a trend toward decreased TAGs and cholesterol esters in plasma. While the data presented here are generally consistent with these previously reported results, there were some important differences in our findings (Figure 5 and Supplemental Figure S4). For example, in mice after CS exposure for 8 months, we observed increased plasma TAGs with long FA carbon chains (49–58) primarily composed of unsaturated and polyunsaturated FAs. While these results differed from previous published data, they were consistent with the clinical chemistry analysis of triglycerides and VLDL in our comprehensive mouse study (Phillips et al., 2016) and, importantly, with historical data showing the impact of cigarette smoking on serum lipids (Craig et al., 1989; Yeung, 1976). Compared with CS, THS2.2 exposure had a more limited effect on plasma TAGs and cessation and switching showed, instead, a trend toward decreased plasma TAGs (Supplemental Figure S4). In addition to effects on TAG levels, we observed a significant increase in free cholesterol in only the 3R4F group, while the other exposure groups showed a tendency toward decreased free cholesterol relative to the sham exposed group. In this regard, the plasma lipid profiles in the 3R4F group matched atherogenic plasma lipidome profiles expected to result from CS exposure and highlighted the lesser effects of THS2.2 aerosol exposure.

Moreover, analysis of the liver proteome and transcriptome showed upregulation of several enzymes involved in FA and cholesterol metabolism specifically in the 3R4F group. While these changes were generally consistent with the plasma lipidomics results, variability in the liver lipidome data made them more challenging to interpret. Interestingly, however, among the molecular changes in liver lipid metabolism, a consistent downregulation of enzymes involved in bile acid metabolism was observed in the 3R4F group. Specifically, we observed a marked reduction of several peroxisomal enzymes (Pipox, Pecr, Hao1 and Hsd17b6) and two important solute carrier proteins (Slc27a2 and Slc27a5) involved in bile acid metabolism (Figure 5C). This was consistent with a report of reduced cholic and chenodeoxycholic acids in the livers of rats exposed to CS for 90 days (Latha et al., 1988).

Besides their importance in bile acid metabolism, peroxisomes are considered crucial organelles in ROS generation, thus contributing to oxidative stress (Schrader & Fahimi, 2006). Indeed, it has been estimated that about 35% of all H_2O_2 formed in the rat liver is produced by peroxisomal oxidases (Boveris et al., 1972). Our findings, especially the increased PEX19 expression in the 3R4F group, suggested increased peroxisome biogenesis with CS exposure. PEX19 is a peroxin protein that, together with PEX3, is among the most important components of the machinery required for early peroxisomal biogenesis (Hattula et al., 2014; Matsuzono et al., 1999; Sacksteder et al., 2000). Consistent with this observation, elevated environmental oxygen concentrations and a variety of xenobiotics were reported to induce a moderate increase in the volume density of peroxisomes and levels of their ROS scavenging enzymes (Schrader & Fahimi, 2006; Van der Valk et al., 1985).

The peroxisome-related changes are likely related to the observation that several antioxidant and xenobiotic metabolism-involved enzymes were upregulated, specifically upon CS exposure. Hence, cytochrome P450 enzymes (CYPs) were upregulated in the livers of the 3R4F group. Importantly, these upregulated CYPs are involved in both lipotoxicity prevention (Cyp4a14 and Cyp4a10) and CS-associated substrate removal (Cyp1a2 and Cyp2a5) (Bartsch et al., 2000; Hsu et al., 2007; Zhou et al., 2010) (Figure 6). In addition, members of the three main hepatic soluble GST families (GSTalpha, Mu and Pi) were upregulated (Figure 6). These soluble GSTs act primarily as detoxification enzymes to prevent oxidative cytotoxic and genotoxic damage (Hayes & McLellan, 1999; Hayes & Pulford, 1995). Again, these effects were much lower with THS2.2 exposure and upon cessation or switching to THS2.2.

The relationship between cigarette smoke and oxidative stress has been long studied, showing a direct connection between CS-derived free radicals and several comorbidities associated with smoking (Aoshiba & Nagai, 2003; Messner & Bernhard, 2014; Zuo et al., 2014). However, while for the respiratory system a direct role of CS in inducing oxidative stress is well known, in the liver a contribution of both direct and indirect CS-related effects seems likely (El-Zayadi, 2006). One possible indirect effect associated with CS exposure and linked to oxidative stress is hepatic iron overload (Gutteridge & Halliwell, 1989). Indeed, CS exposure is associated with tissue hypoxia caused by increased carboxyhemoglobin and the resulting reduction in the oxygen carrying capacity of red blood cells (Rampling, 1993). Hypoxia, in turn, is associated with erythropoietin production and hyperplasia of the bone marrow triggering, as a secondary effect, an increase in red blood cells mass (polycythemia) and turnover. Together, these processes elicit an increased red blood cell-derived iron catabolism leading to

deleterious iron accumulation in hepatocytes and consequent liver cell injury (El-Zayadi, 2006; El-Zayadi et al., 2002; Ghio et al., 2008; Gutteridge & Halliwell, 1989). In support of likely CS effects on liver iron homeostasis, the 3R4F group showed a concomitant increase in red blood cell parameters, hematocrit, erythrocyte counts and hemoglobin and upregulation of several related proteins (Figure 7).

The reduction of CS-related effects with THS2.2 exposure, as well as in the cessation and switching to THS2.2 groups, represents an important finding consistent throughout the entire study. Of note, the latter conditions (cessation and switching) showed similar effects on liver homeostasis, highlighting the possibility that CS-related effects can be reversed. However, for this, it is important to keep in mind that the CS exposure before cessation and switching was relatively short (2 months), which likely did not allow enough time for establishment of longer-term CS effects in liver. Therefore, in future studies, it would be informative to test the reversibility of CS effects after an extended exposure period.

Conclusions

In summary, while signs of overt hepatotoxicity were absent, livers of *Apoe*$^{-/-}$ mice exposed to CS did exhibit specific molecular responses. These included dysregulation of fundamental hepatic processes such as lipid, xenobiotic and possibly iron homeostasis, which were much less affected in the THS2.2, cessation and switching groups. This analysis of liver effects complements the results obtained for respiratory and cardiovascular endpoints within our comprehensive system toxicology assessment study for THS2.2 (Phillips et al., 2016; Titz et al., 2016) and further supports the concept that THS2.2 exposure, as compared with CS, results in reduced biological effects.

Acknowledgements

We thank the members of the bioresearch and aerosol generation teams at PMIRL-S for their technical contributions. We thank Marja Talikka for manuscript revision and scientific discussion.

Declaration of interest

All (except for A.B.) authors are employees of Philip Morris International. Philip Morris International is the sole source of funding and sponsor of this project. GLS and VB are contracted paid by Philip Morris International. A.B. is an employee of Histovia GmbH which was contracted and paid by Philip Morris International to perform the histopathological analysis.

References

Abel J, de Ruiter N. (1989). Inhibition of hydroxyl-radical-generated DNA degradation by metallothionein. Toxicol Lett 47:191–6.

Altamirano J, Bataller R. (2010). Cigarette smoking and chronic liver diseases. Gut 2008:162453

Aoshiba K, Nagai A. (2003). Oxidative stress, cell death, and other damage to alveolar epithelial cells induced by cigarette smoke. Tob Induc Dis 1:219–26.

Arosio P, Yokota M, Drysdale JW. (1976). Structural and immunological relationships of isoferritins in normal and malignant cells. Cancer Res 36:1735–9.

Arunachalam G, Sundar IK, Hwang JW, et al. (2010). Emphysema is associated with increased inflammation in lungs of atherosclerosis-prone mice by cigarette smoke: implications in comorbidities of COPD. J Inflamm (Lond) 7:34

Azzalini L, Ferrer E, Ramalho LN, et al. (2010). Cigarette smoking exacerbates nonalcoholic fatty liver disease in obese rats. Hepatology 51:1567–76.

Bartsch H, Nair U, Risch A, et al. (2000). Genetic polymorphism of CYP genes, alone or in combination, as a risk modifier of tobacco-related cancers. Cancer Epidemiol Biomarkers Prev 9:3–28.

Bonomini F, Rodella L, Moghadasian M, et al. (2013). Apolipoprotein E deficiency and a mouse model of accelerated liver aging. Biogerontology 14:209–20.

Boué S, De León H, Schlage WK, et al. (2013). Cigarette smoke induces molecular responses in respiratory tissues of ApoE−/− mice that are progressively deactivated upon cessation. Toxicology 314: 112–24.

Boué S, Tarasov K, Jänis M, et al. (2012). Modulation of atherogenic lipidome by cigarette smoke in apolipoprotein E-deficient mice. Atherosclerosis 225:328–34.

Boveris A, Oshino N, Chance B. (1972). The cellular production of hydrogen peroxide. Biochem J 128:617–30.

Brown KE, Broadhurst KA, Mathahs MM, Weydert J. (2007). Differential expression of stress-inducible proteins in chronic hepatic iron overload. Toxicol Appl Pharmacol 223:180–6.

Chen J, Bardes EE, Aronow BJ, Jegga AG. (2009). ToppGene Suite for gene list enrichment analysis and candidate gene prioritization. Nucleic Acids Res 37:W305–11.

Church DF, Pryor WA. (1985). Free-radical chemistry of cigarette smoke and its toxicological implications. Environ Health Perspect 64: 111

Craig WY, Palomaki GE, Haddow JE. (1989). Cigarette smoking and serum lipid and lipoprotein concentrations: an analysis of published data. BMJ 298:784–8.

Daly AK, Cholerton S, Armstrong M, Idle JR. (1994). Genotyping for polymorphisms in xenobiotic metabolism as a predictor of disease susceptibility. Environ Health Perspect 102:55–61

De León H, Boué S, Peitsch M, Hoeng J. (2013). Modulation of the hepatic lipidome and transcriptome of Apoe−/−mice in response to smoking cessation. J Liver 2:132.

El-Zayadi AR. (2006). Heavy smoking and liver. World J Gastroenterol 12:6098–101

El-Zayadi AR, Selim O, Hamdy H, et al. (2002). Heavy cigarette smoking induces hypoxic polycythemia (erythrocytosis) and hyperuricemia in chronic hepatitis C patients with reversal of clinical symptoms and laboratory parameters with therapeutic phlebotomy. Am J Gastroenterol 97:1264–5.

Ferdinandusse S, Houten SM. (2006). Peroxisomes and bile acid biosynthesis. Biochim Biophys Acta 1763:1427–40.

Gentleman RC, Carey VJ, Bates DM, et al. (2004). Bioconductor: open software development for computational biology and bioinformatics. Genome Biol 5:R80

Gepner AD, Piper ME, Johnson HM, et al. (2011). Effects of smoking and smoking cessation on lipids and lipoproteins: outcomes from a randomized clinical trial. Am Heart J 161:145–51.

Ghio AJ, Hilborn ED, Stonehuerner JG, et al. (2008). Particulate matter in cigarette smoke alters iron homeostasis to produce a biological effect. Am J Respir Crit Care Med 178:1130–8.

Gutteridge JM, Halliwell B. (1989). Iron toxicity and oxygen radicals. Baillieres Clin Haematol 2:195–256.

Hamabe A, Uto H, Imamura Y, et al. (2011). Impact of cigarette smoking on onset of nonalcoholic fatty liver disease over a 10-year period. J Gastroenterol 46:769–78.

Hassett C, Robinson KB, Beck NB, Omiecinski CJ. (1994). The human microsomal epoxide hydrolase gene (EPHX1): complete nucleotide sequence and structural characterization. Genomics 23: 433–42.

Hattula K, Hirschberg D, Kalkkinen N, et al. (2014). Association between the intrinsically disordered protein PEX19 and PEX3. PLoS One 9:e103101

Hayes JD, Flanagan JU, Jowsey IR. (2005). Glutathione transferases. Annu Rev Pharmacol Toxicol 45:51–88.

Downloaded by [PMP S A], [Bjoern Titz] at 08:38 28 April 2016

Downloaded by [PMP S A], [Bjoern Titz] at 08:38 28 April 2016

Hayes JD, McLellan LI. (1999). Glutathione and glutathione-dependent enzymes represent a co-ordinately regulated defence against oxidative stress. Free Radic Res 31:273–300.

Hayes JD, Pulford DJ. (1995). The glutathione S-transferase supergene family: regulation of GST and the contribution of the lsoenzymes to cancer chemoprotection and drug resistance part II. Crit Rev Biochem Mol Biol 30:521–600.

Helen A, Vijayammal P. (1997). Vitamin C supplementation on hepatic oxidative stress induced by cigarette smoke. J Appl Toxicol 17:289–95.

Hentze MW, Muckenthaler MU, Andrews NC. (2004). Balancing acts: molecular control of mammalian iron metabolism. Cell 117:285–97.

Hsu MH, Savas Ü, Griffin KJ, Johnson EF. (2007). Human cytochrome p450 family 4 enzymes: function, genetic variation and regulation. Drug Metab Rev 39:515–38.

Jung HR, Sylvänne T, Koistinen KM, et al. (2011). High throughput quantitative molecular lipidomics. Biochim Biophys Acta 1811: 925–34.

Kanehisa M, Goto S, Sato Y, et al. (2014). Data, information, knowledge and principle: back to metabolism in KEGG. Nucleic Acids Res 42: D199–205.

Kogel U, Schlage WK, Martin F, et al. (2014). A 28-day rat inhalation study with an integrated molecular toxicology endpoint demonstrates reduced exposure effects for a prototypic modified risk tobacco product compared with conventional cigarettes. Food Chem Toxicol 68:204–17.

Kojima N, Young CR, Bates GW. (1982). Failure of metallothionein to bind iron or act as an iron mobilizing agent. Biochim Biophys Acta 716:273–5.

Koturbash I, Scherhag A, Sorrentino J, et al. (2011). Epigenetic mechanisms of mouse inter-strain variability in genotoxicity of the environmental toxicant 1, 3-butadiene. Toxicol Sci 122:448–56

Latha M, Vijayammal P, Kurup P. (1988). Effect of exposure of rats to cigarette smoke on the metabolism of lipids. Atherosclerosis 70: 225–31.

Lê Cao KA, González I, Déjean S. (2009). integrOmics: an R package to unravel relationships between two omics datasets. Bioinformatics 25: 2855–6.

Liberzon A, Subramanian A, Pinchback R, et al. (2011). Molecular signatures database (MSigDB) 3.0. Bioinformatics 27:1739–40.

Lietz M, Berges A, Lebrun S, et al. (2013). Cigarette-smoke-induced atherogenic lipid profiles in plasma and vascular tissue of apolipoprotein E-deficient mice are attenuated by smoking cessation. Atherosclerosis 229:86–93.

Liu Y, Meyer C, Xu C, et al. (2013). Animal models of chronic liver diseases. Am J Physiol Gastrointest Liver Physiol 304:G449–68.

Lu Y, Ward SC, Cederbaum AI. (2013). Nicotine enhances ethanol-induced fat accumulation and collagen deposition but not inflammation in mouse liver. Alcohol 47:353–7.

Matsuzono Y, Kinoshita N, Tamura S, et al. (1999). Human PEX19: cDNA cloning by functional complementation, mutation analysis in a patient with Zellweger syndrome, and potential role in peroxisomal membrane assembly. Proc Natl Acad Sci USA 96:2116–21.

McCall MN, Bolstad BM, Irizarry RA. (2010). Frozen robust multiarray analysis (fRMA). Biostatistics 11:242–53.

Messner B, Bernhard D. (2014). Smoking and cardiovascular disease: mechanisms of endothelial dysfunction and early atherogenesis. Arterioscler Thromb Vasc Biol 34:509–15.

Moennikes O, Vanscheeuwijck PM, Friedrichs B, et al. (2008). Reduced toxicological activity of cigarette smoke by the addition of ammonia magnesium phosphate to the paper of an electrically heated cigarette: subchronic inhalation toxicology. Inhal Toxicol 20:647–63.

Moon MS, McDevitt E, Zhu J, et al. (2012). Elevated hepatic iron activates NF-E2-related factor 2 (NRF2) regulated pathway in a dietary iron overload mouse model. Toxicol Sci 129:74–85

Mootha VK, Lindgren CM, Eriksson KF, et al. (2003). PGC-1α-responsive genes involved in oxidative phosphorylation are coordinately downregulated in human diabetes. Nat Genet 34:267–73.

Nakashima Y, Plump AS, Raines EW, et al. (1994). ApoE-deficient mice develop lesions of all phases of atherosclerosis throughout the arterial tree. Arterioscler Thromb 14:133–40.

Oppermann U. (2007). Carbonyl reductases: the complex relationships of mammalian carbonyl- and quinone-reducing enzymes and their role in physiology. Annu Rev Pharmacol Toxicol 47:293–322.

Pavek P, Dvorak Z. (2008). Xenobiotic-induced transcriptional regulation of xenobiotic metabolizing enzymes of the cytochrome P450 superfamily in human extrahepatic tissues. Curr Drug Metab 9: 129–43.

Pessione F, Ramond MJ, Njapoum C, et al. (2001). Cigarette smoking and hepatic lesions in patients with chronic hepatitis C. Hepatology 34:121–5.

Phillips B, Veljkovic E, Peck MJ, et al. (2015). A 7-month cigarette smoke inhalation study in C57BL/6 mice demonstrates reduced lung inflammation and emphysema following smoking cessation or aerosol exposure from a prototypic modified risk tobacco product. Food Chem Toxicol 80:328–45.

Phillips B, Veljkovic E, Boué S, et al. (2016). An 8-month systems toxicology inhalation/cessation study in ApoE-/- mice to investigate cardiovascular and respiratory exposure effects of a candidate modified risk tobacco product, THS 2.2, compared with conventional cigarettes. Toxicol Sci 149:411–32

Phillips IR, Dolphin CT, Clair P, et al. (1995). The molecular biology of the flavin-containing monooxygenases of man. Chem Biol Interact 96: 17–32.

Rampling MW. (1993) Clotting factors and rheology: mechanisms of damage and intervention. In: Poulter N, Sever P, Thom S, eds. Cardiovascular disease: risk factors and intervention. Oxford: Radcliffe Medical Press, 201–13

Ritchie ME, Phipson B, Wu D, et al. (2015). limma powers differential expression analyses for RNA-sequencing and microarray studies. Nucleic Acids Res 43:e47

Robinson D, Whitehead T. (1989). Effect of body mass and other factors on serum liver enzyme levels in men attending for well population screening. Ann Clin Biochem 26:393–400.

Rodriguez A, Luukkaala T, Fleming RE, et al. (2009). Global transcriptional response to Hfe deficiency and dietary iron overload in mouse liver and duodenum. PLoS One 4:e7212

Russell DW. (1992). Cholesterol biosynthesis and metabolism. Cardiovasc Drugs Ther 6:103–10.

Sacksteder KA, Jones JM, South ST, et al. (2000). PEX19 binds multiple peroxisomal membrane proteins, is predominantly cytoplasmic, and is required for peroxisome membrane synthesis. J Cell Biol 148: 931–44.

Sauer JM, Hartung T, Leist M, et al. (2015). Systems toxicology: the future of risk assessment. Int J Toxicol 34:346–8.

Schorp MK, Tricker AR, Dempsey R. (2012). Reduced exposure evaluation of an electrically heated cigarette smoking system. Part 1: non-clinical and clinical insights. Regul Toxicol Pharmacol 64: S1–10.

Schrader M, Fahimi HD. (2006). Peroxisomes and oxidative stress. Biochim Biophys Acta 1763:1755–66.

Sheedfar F, Biase SD, Koonen D, Vinciguerra M. (2013). Liver diseases and aging: friends or foes? Aging Cell 12:950–4.

Smith CA, Harrison DJ. (1997). Association between polymorphism in gene for microsomal epoxide hydrolase and susceptibility to emphysema. Lancet 350:630–3.

Sturla SJ, Boobis AR, FitzGerald RE, et al. (2014). Systems toxicology: from basic research to risk assessment. Chem Res Toxicol 27: 314–29.

Subramanian A, Tamayo P, Mootha VK, et al. (2005). Gene set enrichment analysis: a knowledge-based approach for interpreting genome-wide expression profiles. Proc Natl Acad Sci USA 102: 15545–50.

Szklarczyk D, Franceschini A, Wyder S, et al. (2015). STRING v10: protein-protein interaction networks, integrated over the tree of life. Nucleic Acids Res 43:D447–52.

Tao Y, Wu Q, Guo X, et al. (2014). MBD5 regulates iron metabolism via methylation-independent genomic targeting of Fth1 through KAT2A in mice. Br J Haematol 166:279–91.

Terpstra PM, Teredesai A, Vanscheeuwijck PM, et al. (2003). Toxicological evaluation of an electrically heated cigarette. Part 4: subchronic inhalation toxicology. J Appl Toxicol 23:349–62.

Thomas C, Mackey MM, Diaz AA, Cox DP. (2009). Hydroxyl radical is produced via the Fenton reaction in submitochondrial particles under oxidative stress: implications for diseases associated with iron accumulation. Redox Rep 14:102–8.

Thornalley PJ, Vašák M. (1985). Possible role for metallothionein in protection against radiation-induced oxidative stress. Kinetics and mechanism of its reaction with superoxide and hydroxyl radicals. Biochim Biophys Acta 827:36–44.

Titz B, Boué S, Phillips B, et al. (2016). Effects of cigarette smoke, cessation and switching to two heat-not-burn tobacco products on lung lipid metabolism in C57BL/6 and Apoe−/− mice – an integrative systems toxicology analysis. Toxicol Sci 149:441–57

Titz B, Elamin A, Martin F, et al. (2014). Proteomics for systems toxicology. Comput Struct Biotechnol J 11:73–90.

Tsochatzis E, Papatheodoridis GV, Manolakopoulos S, et al. (2009). Smoking is associated with steatosis and severe fibrosis in chronic hepatitis C but not B. Scand J Gastroenterol 44:752–9.

U.S. Department of Health and Human Services. (2010). How tobacco smoke causes disease: the biology and behavioral basis for smoking-attributable disease: a report of the surgeon general. Atlanta, GA: U.S. Department of Health and Human Services, Centers for Disease Control and Prevention, National Center for Chronic Disease Prevention and Health Promotion, Office on Smoking and Health

Van der Valk P, Gille J, Oostra A, et al. (1985). Characterization of an oxygen-tolerant cell line derived from Chinese hamster ovary. Cell Tissue Res 239:61–8.

Väremo L, Nielsen J, Nookaew I. (2013). Enriching the gene set analysis of genome-wide data by incorporating directionality of gene expression and combining statistical hypotheses and methods. Nucleic Acids Res 41:4378–91.

Vizcaíno JA, Deutsch EW, Wang R, et al. (2014). ProteomeXchange provides globally coordinated proteomics data submission and dissemination. Nat Biotechnol 32:223–6.

Werley MS, Freelin SA, Wrenn SE, et al. (2008). Smoke chemistry, in vitro and in vivo toxicology evaluations of the electrically heated cigarette smoking system series K. Regul Toxicol Pharmacol 52: 122–39.

Whitehead T, Robinson D, Allaway S. (1996). The effects of cigarette smoking and alcohol consumption on serum liver enzyme activities: a dose-related study in men. Ann Clin Biochem 33:530–5.

Yeung D. (1976). Relationships between cigarette smoking, oral contraceptives, and plasma vitamins A, E, C, and plasma triglycerides and cholesterol. Am J Clin Nutr 29:1216–21.

Young CJ, Moss J. (1989). Smoke inhalation: diagnosis and treatment. J Clin Anesth 1:377–86.

Yu MW, Hsu FC, Sheen IS, et al. (1997). Prospective study of hepatocellular carcinoma and liver cirrhosis in asymptomatic chronic hepatitis B virus carriers. Am J Epidemiol 145:1039–47.

Zein CO, Beatty K, Post AB, et al. (2006). Smoking and increased severity of hepatic fibrosis in primary biliary cirrhosis: a cross validated retrospective assessment. Hepatology 44:1564–71.

Zein CO, Unalp A, Colvin R, et al. (2011). Smoking and severity of hepatic fibrosis in nonalcoholic fatty liver disease. J Hepatol 54: 753–9.

Zevin S, Benowitz NL. (1999). Drug interactions with tobacco smoking. Clin Pharmacokinet 36:425–38.

Zhang SH, Reddick RL, Piedrahita JA, Maeda N. (1992). Spontaneous hypercholesterolemia and arterial lesions in mice lacking apolipoprotein E. Science 258:468–71.

Zhou X, Zhuo X, Xie F, et al. (2010). Role of CYP2A5 in the clearance of nicotine and cotinine: insights from studies on a Cyp2a5-null mouse model. J Pharmacol Exp Ther 332:578–87.

Zuo L, He F, Sergakis GG, et al. (2014). Interrelated role of cigarette smoking, oxidative stress, and immune response in COPD and corresponding treatments. Am J Physiol Lung Cell Mol Physiol 307: L205–18.

Supplementary material available online

Supplementary Figures S1–S8, and Tables S1 and S2

Downloaded by [PMP S A], [Bjoern Titz] at 08:38 28 April 2016